Integrative Medicine Research

journal homepage: www.imr-journal.com

Original Article

Numerical reproduction of hemodynamics change by acupuncture on Taichong (LR-3) based on the lumped-parameter approximation model of the systemic arteries

Atsushi Shirai[a,*], *Takuya Suzuki*[b], *Takashi Seki*[c]

[a] *Institute of Fluid Science, Tohoku University, Miyagi, Japan*
[b] *Graduate School of Biomedical Engineering, Tohoku University, Miyagi, Japan*
[c] *Division of Geriatric Behavioral Neurology, Tohoku University CYRIC, Miyagi, Japan*

ARTICLE INFO

Article history:
Received 12 February 2015
Received in revised form
23 June 2015
Accepted 26 June 2015
Available online 6 July 2015

Keywords:
acupuncture
hemodynamics
lumped-parameter approximation
modeling
systemic vascular resistance

ABSTRACT

Background: The aim of this study was to develop a mathematical model of blood flow in the systemic circulation to emulate the change in hemodynamics by acupuncture therapy to elucidate the mechanism of the therapy. For this purpose, as a first step, a simple model of arterial blood flow was presented to reproduce previously reported change in the blood flow volume by the acupuncture needle stimulation of Taichong (LR-3).

Methods: This model was based on the lumped-parameter approximation of arterial blood flow together with linear resistance of peripheral circulation. It has been reported that blood flow in the left arm was enhanced after the stimulation, yielding the peripheral vascular resistance-regulated blood flow dominated by the sympathetic nervous system. In addition to the peripheral resistance, another parameter that possibly regulates the blood flow is the cross-sectional area of the vessel. These two factors were changed to numerically examine their contributions to the blood flow based on the hypothesis that they could be changed by the stimulation. The numerical result was compared with the experimental result to confirm the validity of the hypothesis that the blood flow in the arm is regulated by the peripheral resistance.

Results: This model is extremely simple and the physical parameters introduced for the simulation were gleaned from different reports in the literature. It was demonstrated, however, that regulation of the peripheral resistance rather than of the cross-sectional area could reproduce the experimentally observed change in the blood flow. Moreover, the relationship between the changes in the flow volume and the systemic vascular resistance quantitatively matched the experimental data.

Conclusion: The present model has a potential to emulate hemodynamic change by acupuncture therapy by incorporating physiological correlation of stimulation of an acupoint and regulation of parameters that affect the hemodynamics.

* *Corresponding author*. Institute of Fluid Science, Tohoku University, 2-1-1 Katahira, Aoba-ku, Sendai, Miyagi 980-8577, Japan.
E-mail address: shirai@ifs.tohoku.ac.jp (A. Shirai).

http://dx.doi.org/10.1016/j.imr.2015.06.003

1. Introduction

Acupuncture therapy is an important component of traditional Chinese medicine along with moxibustion and herbal medicine. In traditional Chinese medicine, it is believed that a meridian network is spread over the entire human body and that "Qi" or "blood" runs over the meridians to maintain life.[1] Acupuncture involves restoration of the normal flow of Qi or blood by stimulating appropriate "acupoints," about 400 of which exist in the human body, using needles (acupuncture needles).

Recently, the effectiveness of acupuncture therapy has been reported from a modern medical point of view. For example, in a randomized controlled trial of patients suffering from chronic neck pain, the symptoms of patients receiving additional acupuncture improved faster than those receiving only primary care.[2] Witt et al[3–6] reported randomized acupuncture trials in patients with osteoarthritis of the knee, migraine, tension-type headache, and chronic low back pain. In those studies, acupuncture was found to be more effective in patients with some types of pain, compared with those who did not receive any treatment. Yamazaki et al[7] showed that acupuncture could enhance cognitive function and possibly prevent dementia. In 1999, *Guidelines on basic training and safety in acupuncture* was published by the World Health Organization,[8] and the therapy has been approved for treatment of various diseases including diseases of the nervous system. Therefore, currently in the United States, Europe, and Asia, acupuncture is being used together with modern medicine in actual medical practice.[1,9,10]

Acupuncture therapy, however, presently lacks a scientific basis because its body of the theory is based on the existence of hypothetical organs and the concept of meridians, acupoints, and Qi that cannot yet be validated by modern medicine and science. Thus, the distrust of acupuncture therapy cannot be easily dispelled. Therefore, scientific elucidation of underlying acupuncture mechanism is essential for the therapy to be generally accepted in the future. There are only few studies in which quantitative measurement of blood flow in response to stimulation of a specific acupoint was conducted at clinical sites[11–13]; whereas, numerous studies were conducted on hemodynamic change following acupuncture therapy. Takayama et al[11] measured blood pressure (BP), cardiac index (CI) and systemic vascular resistance index (SVRI), and the diameter and blood flow volume of left brachial and radial arteries in response to acupuncture therapy applied to Taichong (LR-3), focusing on the effect of the stimulation of the acupoint on the hemodynamics. The authors of that study demonstrated that blood flow volume in the arm decreased during twisting of the acupuncture needle and then increased to a level higher than the preacupuncture level at 180 seconds after the stimulation, while BP and CI were not changed. They also demonstrated that SVRI at 180 seconds after the stimulation was decreased. Vasoconstriction of digital blood vessels, unlike the case of other vessels, is regulated only by the sympathetic nervous system,[14] and change in peripheral blood circulation at the fingernail bed by acupuncture has been reported.[15] Therefore, Takayama et al[11] argued that the steep decrease and subsequent gradual increase in the blood flow volume were due to the change in peripheral vascular resistance induced by tension and sedation of the sympathetic nervous system.

It is difficult to noninvasively observe the correlation between stimulation of an acupoint and the change in peripheral vascular resistance other than presuming it from resultant change in the flow volume or SVRI in response to the stimulation. Numerical simulation is expected to provide additional information not only for evaluating the contribution of the change in the vascular resistance to the hemodynamics, but also for systemic elucidation of the mechanism of the therapy in future by combining it with a correlation model of stimulation and the physiological parameters. In this study, as an initial step, a simple mathematical model of blood flow in a systemic arterial system was presented to reproduce the changes in the blood flow by stimulation of Taichong.[11] The arterial system was simplified to the aorta, arteries of the four limbs, and the superior mesenteric artery. Blood flow in each artery was expressed by the lumped-parameter approximation and each peripheral circulation was modeled as a linear resistance. Cross-sectional area of the artery of the left arm and its peripheral vascular resistance were chosen as parameters that affect the blood flow in the arm, and they were changed to investigate their contributions to the blood flow. The result of this study was compared with that of Takayama et al[11] to confirm the validity of their hypothesis that the blood flow is dominated by the peripheral vascular resistance of that arm.

2. Methods

2.1. *Lumped-parameter approximation model*

Fig. 1 shows a schematic of the lumped-parameter approximation model of the systemic arterial system introduced in this study. This model consists of arteries modeled by straight rigid pipes, with each peripheral circulation being modeled by a linear resistance. The upstream end of the model is connected to the left ventricle. Each artery is defined as a part divided by points of pressure definition points, P_S and P_1–P_8. The arteries are numbered as follows: Number 1 is the ascending aorta and the aortic arch, Number 2 extends from the subclavian artery to the radial artery of the left arm, Number 3 extends from the brachiocephalic artery to the radial artery of the right arm, Number 4 is the thoracic aorta and the abdominal aorta above the branching of the superior mesenteric artery, Number 5 is the superior mesenteric artery, Number 6 is the remaining portion of the abdominal aorta below the branching of the super mesenteric artery, Number 7 extends from the common iliac artery to the anterior tibial artery of the left leg, and Number 8 extends from the common iliac artery to the anterior tibial artery of the right leg. These arteries were chosen by referring to major branches of canine arterial tree.[16] Pressures are defined at both ends of each artery, and flow volume is defined at the middle assuming that the blood flows uniformly. Table 1 presents the length L, proximal radius R_u, and distal radius R_d of the arteries.[17,18]

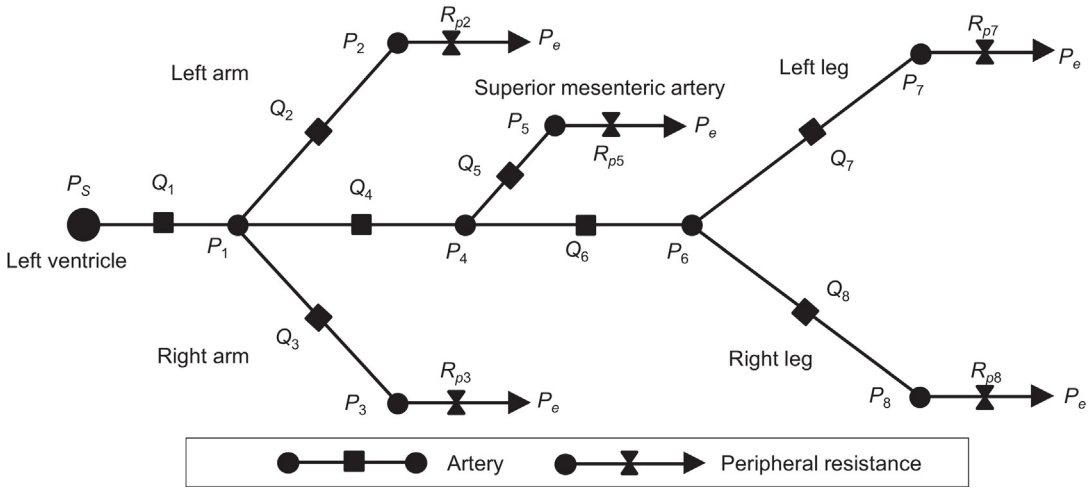

Fig. 1 – Schematic of arterial system model. Pressure is defined at circles and flow volume is defined at squares.

2.2. *Governing equations*

Blood is assumed to be an incompressible Newtonian fluid with viscosity (μ) of 3.5×10^{-3} Pa·s (3.5 cP), which was chosen as an intermediate value between 3.0×10^{-3} Pa·s (3.0 cP) and 4.0×10^{-3} Pa·s (4.0 cP)[19,20]; the flow is laminar steady flow. Neglecting the influence of gravity, the relationship between flow volume Q and pressure difference P_u–P_d of each artery is expressed as follows:

$$Q_i = \frac{A_i^2}{8\pi\mu L_i}\left(P_{u_i} - P_{d_i}\right) \tag{1}$$

where the subscript i represents the ID of an artery listed in Table 1; P_u and P_d are pressures at the proximal and the distal ends of the artery, respectively, and A_i is the mean cross-sectional area of the artery. A_i is obtained using the following equation as the cross-sectional area of a straight cylinder with the same length and volume as the artery modeled as a circular truncated cone:

$$A_i = \frac{\pi}{3}\left(R_{u_i}^2 + R_{u_i}R_{d_i} + R_{d_i}^2\right) \tag{2}$$

The equation of continuity is expressed as follows to denote that inflow and outflow volumes are equal at each junction of arteries:

$$\sum_{i \in J} Q_i = 0 \tag{3}$$

where J is the set of IDs of arteries sharing a pressure definition point P_j.

The pressure drop across a peripheral circulation ΔP is expressed as follows, taking into account its resistance R_p:

$$\Delta P = P_{d_i} - P_e = R_{p_i}Q_i \tag{4}$$

The peripheral vascular resistance was estimated to be 4.3×10^9 Pa·s/m^3 from the pressure difference between an artery and a venule.[21,22] Because it could be an overestimated value due to pressure drops within the artery or in the venule, R_p in this model was assumed to be 1.0×10^9 Pa·s/m^3 for each peripheral circulation to prevent extraordinary laterality of blood distribution. Venous pressure downstream of the peripheral circulation, P_e, was set to 0 Pa considering the facts that pressure at the right atrium is 6 mmHg or less and pulsation of the pressure in venules is much smaller than that in

Table 1 – Size of arteries introduced in the present model[17,18]

Artery ID	Artery	Length (L), m	Proximal radius (R_u), m	Distal radius (R_d), m
1	Ascending aorta–Aortic arch	0.099	0.0147	0.0107
2	Left subclavian artery–Left radial artery	0.691	0.0042	0.0014
3	Brachiocephalic artery–Right radial artery	0.725	0.0062	0.0014
4	Thoracic aorta–Abdominal aorta	0.229	0.0100	0.0059
5	Superior mesenteric artery	0.059	0.0044	0.0044
6	Abdominal aorta	0.116	0.0058	0.0052
7	Left common iliac artery–Left anterior tibial artery	0.988	0.0037	0.0013
8	Right common iliac artery–Right anterior tibial artery	0.992	0.0037	0.0013

Data were gleaned from the reports by Stergiopulos et al[17] and Wang and Paker[18].

Table 2 – Nomenclature

Notation	Description
A	Mean cross-sectional area [Eq. (2)]
L	Length of artery
P_d	Distal pressure of artery
P_e	Venous pressure
P_S	Supply pressure
P_u	Proximal pressure of artery
Q	Flow volume
R_d	Distal radius of artery
R_p	Peripheral vascular resistance
R_u	Proximal radius of artery
μ	Viscosity of blood

the aorta.[23,24] Nomenclatures used in the governing equations are listed in Table 2.

In this study, the contributions of the cross-sectional area of the artery of the left arm, A_2, and its peripheral vascular resistance, R_{p2}, to blood distribution in the body were examined numerically. For this purpose, blood distribution to the arteries was first obtained using the values listed in Table 1 as the control condition, and A_2 and R_{p2} were changed in the range of ±25% from their original values to examine the hemodynamic change from the control condition. Takayama et al[11] showed that neither BP nor cardiac output (CO) was changed through the therapy. It is mathematically impossible, however, to use both supply pressure and supply flow volume simultaneously as the upstream boundary condition. Therefore, the authors conducted the aforementioned simulations by applying a constant pressure of $P_S = 13.3$ kPa (100 mmHg), which corresponds to the mean pressure of the left ventricle,[23,24] and a constant flow volume of $Q_1 = 8.33 \times 10^{-5}$ m^3/s (5 L/min), which corresponds to CO,[25–27] as the upstream boundary condition to examine the influence of the boundary condition on the blood distribution.

2.3. *Systemic vascular resistance*

Takayama et al[11] introduced SVRI as a parameter to discuss hemodynamics. SVRI (dyn·s·m^2/cm^5) is obtained using the following equation with CI (L/min/m^2), mean arterial pressure (MAP, mmHg), and central venous pressure (CVP, mmHg)[28,29]:

$$\mathrm{SVRI} = \frac{\mathrm{MAP} - \mathrm{CVP}}{\mathrm{CI}} \times 80 \quad (5)$$

where CI is the CO (L/min) normalized by body surface area (m^2). In this study, systemic vascular resistance (SVR, MPa·s/m^3), expressed in Eq. (6), is introduced as the representative of Eq. (5) so that the body surface area need not be taken into account[29]:

$$\mathrm{SVR} = \frac{\mathrm{MAP} - \mathrm{CVP}}{\mathrm{CO}} \times 8 \quad (6)$$

Actually, in this model, P_S (Pa) is substituted for MAP, P_e (0 Pa) for CVP, and Q_1 (m^3/s) for CO, and thus, Eq. (6) is rewritten as follows:

$$\mathrm{SVR} = \frac{P_S}{Q_1} \quad (7)$$

3. Results

3.1. *Pressure boundary condition*

Table 3 presents the data on pressure at each definition point, the pressure drop across each artery segment, the flow volume in each segment, and the relative flow volume to Q_1 when a constant pressure of $P_S = 13.3$ kPa (100 mmHg),[23,24] which corresponds to mean BP in the left ventricle, is applied to the upstream end of artery Number 1. Here, $Q_1 = 6.07 \times 10^{-5}$ m^3/s (3.64 L/min), which is in the range of the systemic circulation between 5.60×10^{-5} m^3/s (3.36 L/min) and 7.78×10^{-5} m^3/s (4.67 L/min), which were calculated taking into account the CO at rest ranging from 6.83×10^{-5} m^3/s (4.1 L/min) to 9.50×10^{-5} m^3/s (5.7 L/min)[25–27] and distributions to cerebral and cardiovascular circulations of about 14% and 4%, respectively, of the CO.[30] This result, accordingly, indicates that 1.0×10^9 Pa·s/m^3 of the peripheral vascular resistance is an acceptable value. The resultant SVR in this condition is 219 MPa s/m^3. The flow volume in the left arm, Q_2, is 1.23×10^{-5} m^3/s and the pressure drop across the artery, P_1–P_2, is 1046 Pa, which are focused on hereafter. The hemodynamics is discussed as the change from the values shown in this table.

Fig. 2 shows the changes in each value of pressure and flow volume when the cross-sectional area, A_2, of the left arm was changed in the range of ±25% with its peripheral vascular resistance, R_{p2}, being fixed at the control condition. In Fig. 2A, P_S remains constant because it is the given value. P_2 decreases by 5.8% for a 25% decrease of A_2 and increases by 2.9% for a 25% increase of A_2, whereas P_1 and P_3–P_8 are independent of the change in A_2. In Fig. 2B, Q_1 and Q_2 decrease by 1.2% and 5.8%, respectively, for the 25% decrease of A_2 and increase by 0.59% and 2.9%, respectively, for the 25% increase of A_2, whereas Q_3–Q_8 are independent of the change in A_2. Fig. 3 shows the change in each pressure and flow volume when R_{p2}

Table 3 – Blood distribution at the control condition shown in Table 1 under the pressure boundary condition

Pressure (Pa)	Artery ID	Pressure drop (Pa)	Flow volume (m^3/s)	Ratio from Q_1 (%)
P_1 13,298	1	P_S–P_1 2.0	Q_1 6.07×10^{-5}	100
P_2 12,252	2	P_1–P_2 1,046.0	Q_2 1.23×10^{-5}	20.2
P_3 12,984	3	P_1–P_3 313.5	Q_3 1.30×10^{-5}	21.4
P_4 13,281	4	P_1–P_4 17.3	Q_4 3.55×10^{-5}	58.4
P_5 13,262	5	P_4–P_5 18.6	Q_5 1.33×10^{-5}	21.9
P_6 13,256	6	P_4–P_6 25.0	Q_6 2.22×10^{-5}	36.6
P_7 11,098	7	P_6–P_7 2,157.6	Q_7 1.12×10^{-5}	18.3
P_8 11,091	8	P_6–P_8 2,164.9	Q_8 1.12×10^{-5}	18.3

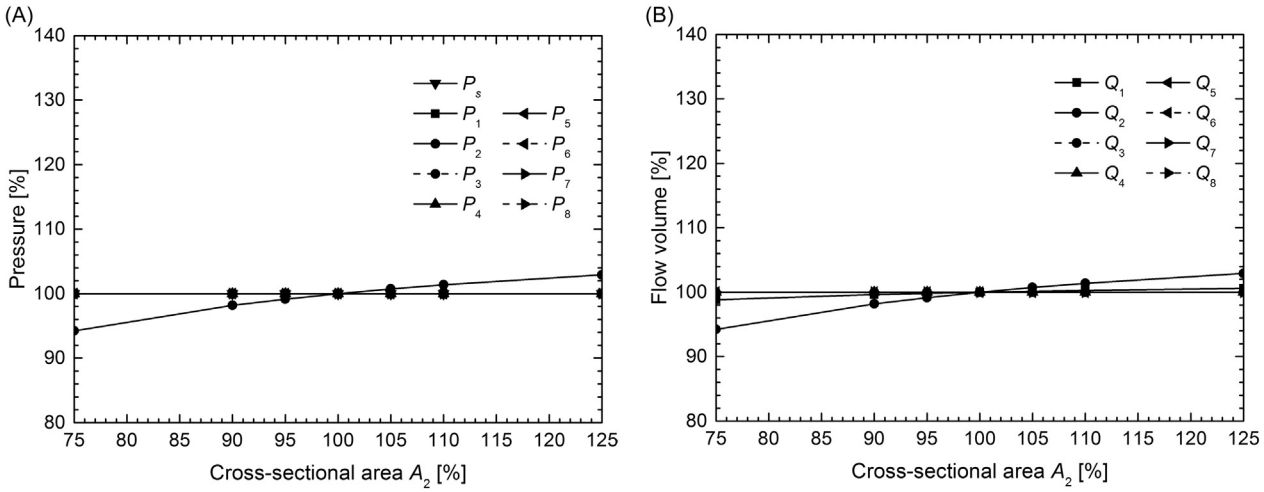

Fig. 2 – Contribution of cross-sectional area of the left arm, A_2, to blood flow under the pressure boundary condition. Tangential axis is the ratio of A_2 from its control condition. (A) Pressure; (B) flow volume.

was changed in the range of ±25% with A_2 being fixed at the control condition. In Fig. 3A, P_2 decreases by 2.6% for a 25% decrease of R_{p2} and increases by 1.6% for a 25% increase of R_{p2}, whereas P_1 and P_3–P_8 are independent of the change in R_{p2}. In Fig. 3B, Q_1 and Q_2 increase by 6.0% and 29.9%, respectively, for the 25% decrease of R_{p2}, and decrease by 3.8% and 18.7%, respectively, for the 25% increase of R_{p2}, whereas Q_3–Q_8 are independent of the change in R_{p2}.

From these results, it can be said that the influence of R_{p2} on the change in Q_2 is more significant than the changes in others. It is interesting that these changes only had an influence on the blood flow in artery Numbers 1 and 2, but not in artery Numbers 3–8.

3.2. *Flow-volume boundary condition*

It was described in the previous section that Q_1 changed with the changes in A_2 or R_{p2} although no statistically significant change in the CO was found in the experiment by Takayama et al.[11] Therefore, in this section, a constant flow volume Q_1 is applied instead of P_S to the upstream boundary.

Table 4 presents the data on the pressure at each definition point, the pressure drop across each artery segment, the flow volume in each segment, and the relative flow volume to Q_1 when a constant flow volume of $Q_1 = 8.33 \times 10^{-5}$ m^3/s (5 L/min),[25–27] which corresponds to CO, is applied at artery Number 1. Here, P_S is 18,256 Pa (137 mmHg), which is higher than the mean BP of 13.3 kPa due to higher Q_1 than that calculated in the previous section. The flow volume in the left arm, Q_2, is 1.68×10^{-5} m^3/s and the pressure drop across the artery, P_1–P_2, is 1,435.8 Pa, which are focused on hereafter. Although these are higher than the values presented in Table 3, it was confirmed that the relative flow volume to Q_1 and SVR was the same. The hemodynamics is discussed as the change from the values shown in Table 4.

Fig. 4 shows the changes in each pressure and flow volume when A_2 was changed in the range of ±25% with R_{p2} being fixed in the control condition. In Fig. 4A, P_2 decreases by 4.1% for a

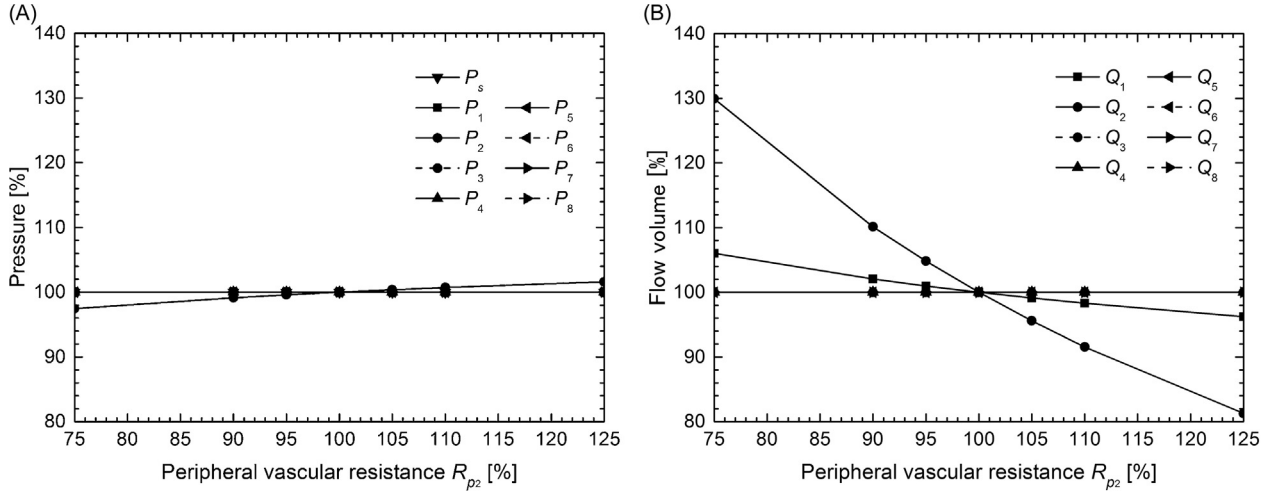

Fig. 3 – Contribution of peripheral vascular resistance of the left arm, R_{p2}, to blood flow under the pressure boundary condition. Tangential axis is the ratio of R_{p2} from its control condition. (A) Pressure; (B) flow volume.

Table 4 – Blood distribution at the control condition shown in Table 1 under the flow-volume boundary condition

Pressure (Pa)	Artery ID	Pressure drop (Pa)	Flow volume (m^3/s)	Ratio from Q_1 (%)
P_1 18,253	1	P_S–P_1 2.78	Q_1 8.33×10^{-5}	100.0
P_2 16,817	2	P_1–P_2 1,435.8	Q_2 1.68×10^{-5}	20.2
P_3 17,823	3	P_1–P_3 430.3	Q_3 1.78×10^{-5}	21.4
P_4 18,229	4	P_1–P_4 23.8	Q_4 4.87×10^{-5}	58.4
P_5 18,204	5	P_4–P_5 25.5	Q_5 1.82×10^{-5}	21.9
P_6 18,195	6	P_4–P_6 34.3	Q_6 3.05×10^{-5}	36.6
P_7 15,233	7	P_6–P_7 2,961.6	Q_7 1.52×10^{-5}	18.3
P_8 15,233	8	P_6–P_8 2,971.6	Q_8 1.52×10^{-5}	18.3

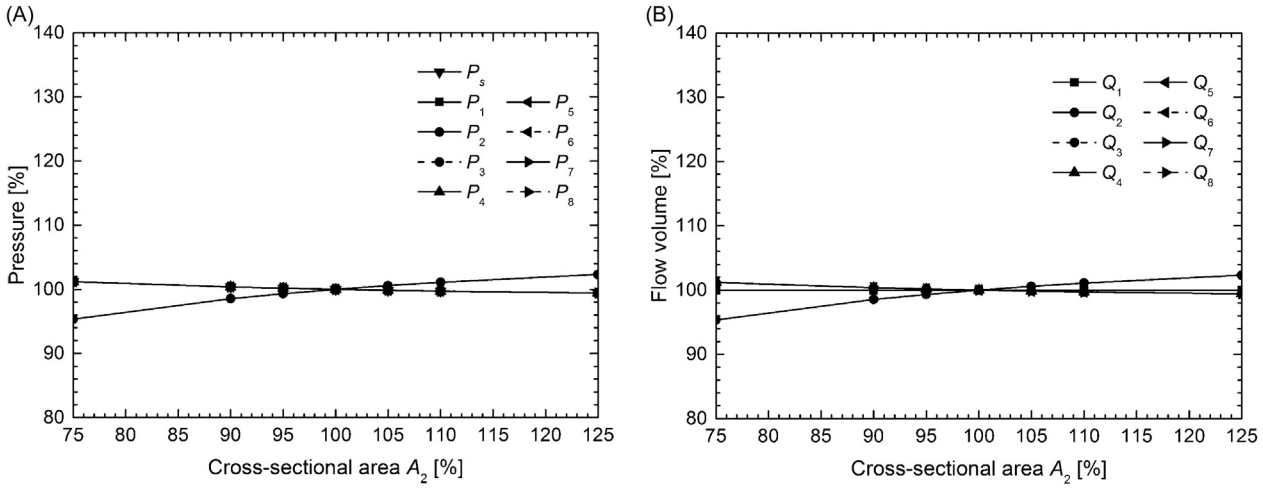

Fig. 4 – Contribution of cross-sectional area of the left arm, A_2, to blood flow under the flow-volume boundary condition. Tangential axis is the ratio of A_2 from its control condition. (A) Pressure; (B) flow volume.

25% decrease of A_2 and increases by 2.0% for a 25% increase of A_2, whereas P_S, P_1, and P_3–P_8 increase by 1.0% for the 25% decrease of A_2 and decrease by 0.58% for the 25% increase of A_2. In Fig. 4B, Q_1 remains constant because it is the given value. Q_2 decreases by 4.1% for the 25% decrease of A_2 and increases by 2.0% for the 25% increase of A_2, whereas Q_3–Q_8 increase by 1.0% for the 25% decrease of A_2 and decrease by 0.58% for the 25% increase of A_2. Fig. 5 shows the change in each pressure and flow volume when R_{p2} was changed in the range of ±25% with A_2 being fixed at the control condition. In Fig. 5A, P_2 decreases by 7.9% for a 25% decrease of R_{p2} and increases by 5.4% for a 25% increase of R_{p2}, whereas P_S, P_1, and P_3–P_8 decrease by 5.8% for the 25% decrease of R_{p2} and increase by 4.0% for the 25% increase of R_{p2}. In Fig. 5B, Q_2 increases by 22.8% for the 25% decrease of R_{p2} and decreases by 15.7% for the 25% increase of R_{p2}, whereas Q_3–Q_8 decrease by 5.8% for the 25% decrease of R_{p2} and increase by 4.0% for the 25% increase of R_{p2}.

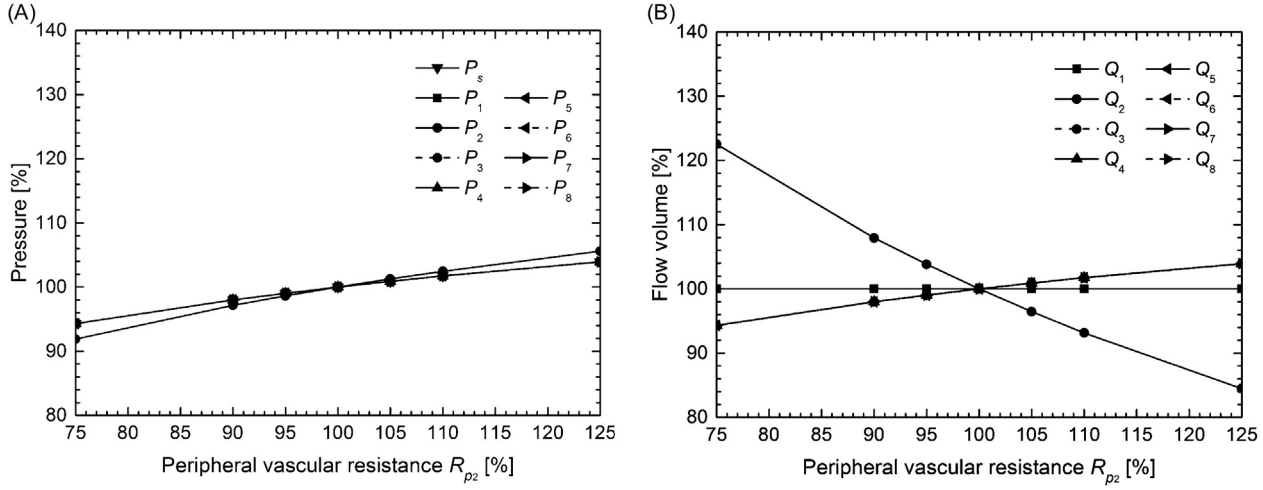

Fig. 5 – Contribution of peripheral vascular resistance of the left arm, R_{p2}, to blood flow under the flow-volume boundary condition. Tangential axis is the ratio of R_{p2} from its control condition. (A) Pressure; (B) flow volume.

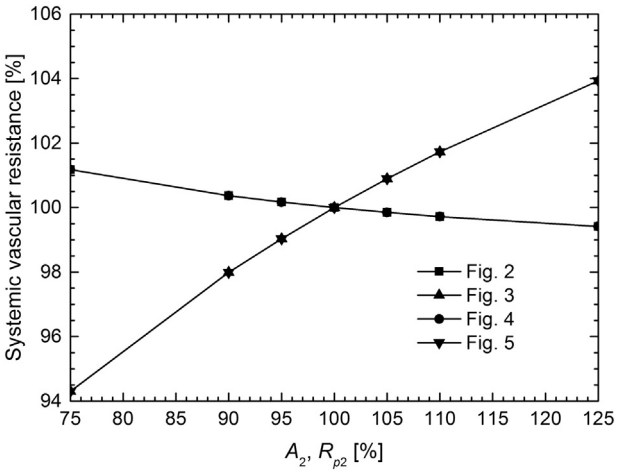

Fig. 6 – Dependence of systemic vascular resistance, SVR, on cross-sectional area, A_2, and peripheral vascular resistance, R_{p2}, of the left arm. A_2 was changed in Figs. 2 and 4, and R_{p2} was changed in Figs. 3 and 5.

Comparing these results with those presented in the previous section, a similar tendency is observed, that is, the influence of R_{p2} on the change in Q_2 is more significant, but the area of influence is different. That is, with the constant supply flow volume, changes in A_2 and R_{p2} influence all the parameters other than Q_1 although the area of influence was limited to Arteries 1 and 2 for the constant supply pressure.

3.3. *Systemic vascular resistance*

Fig. 6 shows the dependence of SVR calculated from Figs. 2–5 on A_2 and R_{p2}. The vertical axis represents the ratio of SVR from 219 MPa s/m^3 at the control condition, and the horizontal axis represents the ratios of A_2 and R_{p2} from their control values (it is the ratio of A_2 in Figs. 2 and 4 and the ratio of R_{p2} in Figs. 3 and 5). From this figure, it can be seen that the change in SVR is independent of the upstream boundary condition. SVR increases by 1.2% for a 25% decrease of A_2 and decreases by 0.58% for a 25% increase of A_2. It decreases by 5.7% for a 25% decrease of R_{p2} and increases by 3.9% for a 25% increase of R_{p2}. This figure indicates that the contribution of R_{p2} to blood flow is superior to that of A_2.

4. Discussion

4.1. *Influence of A_2 and R_{p2} on hemodynamics*

When the cross-sectional area, A_2, of the left arm was changed in the range of ±25% with its peripheral vascular resistance, R_{p2}, being fixed, the magnitude of the corresponding change in the pressures and the flow volumes was up to 5.8% under the pressure boundary condition, as shown in Fig. 2, and up to 4.7% under the flow-volume boundary condition, as shown in Fig. 4. Because they are much smaller than the change in A_2, it can be said that the cross-sectional area contributes less to the blood flow regardless of the upstream boundary condition. Actually, the changes in the pressures and the flow volumes calculated with the present model were less than 1%, corresponding to the maximum change in the cross-sectional area of 3.5% observed by Takayama et al.[11]

By contrast, when R_{p2} was changed in the range of ±25% with A_2 being fixed, the magnitude of the change in Q_2 was 29.9%, whereas those of pressures and other flow volumes were up to 6.0% under the pressure boundary condition, as shown in Fig. 3. The magnitude of the change in Q_2 was 22.5%, whereas those of pressures and other flow volumes were up to 8.1% under the flow-volume boundary condition, as shown in Fig. 5. This result indicates that the influence of R_{p2} on Q_2 is more significant than the others, and thus, it supports the hypothesis by Takayama et al[11] (i.e., the peripheral vascular resistance dominantly regulates the blood flow in the brachial and radial arteries). Together with this fact, because the vasoconstriction of fingers is regulated only by the sympathetic nervous system,[14] the hemodynamics can be said to be regulated by the peripheral vascular resistance controlled by the tension and sedation of the sympathetic nervous system.

4.2. *Comparison of SVR with experimental data*

The maximum magnitude of the change in SVR was 5.7% for a ±25% change in R_{p2} and 1.2% for the same amount of change in A_2, regardless of the upstream boundary condition. This result indicates that the increase in SVR is also due to the increase in the peripheral vascular resistance, which supports the hypothesis by Takayama et al.[11] The reason why SVR is independent of the upstream boundary conditions is explained as follows: Assuming the arterial system shown in Fig. 1 to be one vessel, the relationship between the pressure drop across the vessel, ΔP, and flow volume in it, Q, is expressed as follows using the resistance, R

$$\Delta P = RQ \tag{8}$$

R is expressed as follows because all the venous pressures, P_e, were fixed to 0 Pa in this study.

$$R = \frac{P_S}{Q_1} \tag{9}$$

Because SVR = P_S/Q_1 as shown in Eq. (7), SVR equals R independent of the upstream boundary conditions. This indicates that SVR is uniquely specified by the configuration of the arterial system, including the peripheral vascular resistances.

Fig. 7 shows the dependence of Q_2 on SVR when R_{p2} was changed under the pressure and the flow-volume boundary conditions. SVR in this figure represents the ratio from the value at the control condition. SVRI decreased by 4.3% and the flow volume in the radial artery increased by 19.6% at 180 seconds after the stimulation, as shown in Table 5.[11] In Fig. 7, a 4% decrease in SVR correlates with an increase of about 21% in Q_2 for the pressure boundary condition and an increase of about 16% for the flow-volume boundary condition. The numerical result well agrees with the experimental result despite the size of each artery and the value of the peripheral vascular resistance being based on different reports in the literature. Therefore, this result indicates that the present model

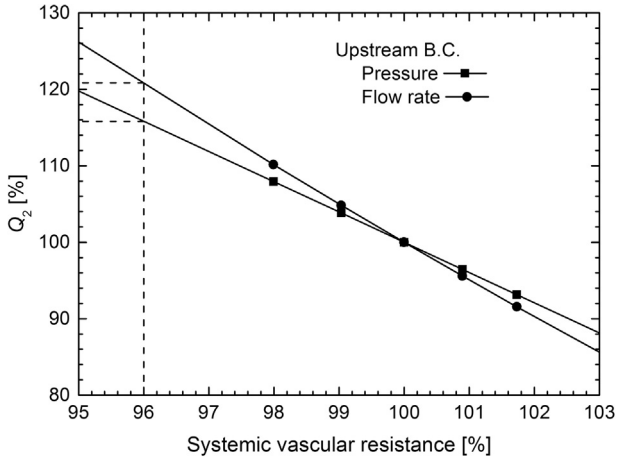

Fig. 7 – Contribution of systemic vascular resistance, SVR, to flow volume in the left arm, Q_2.

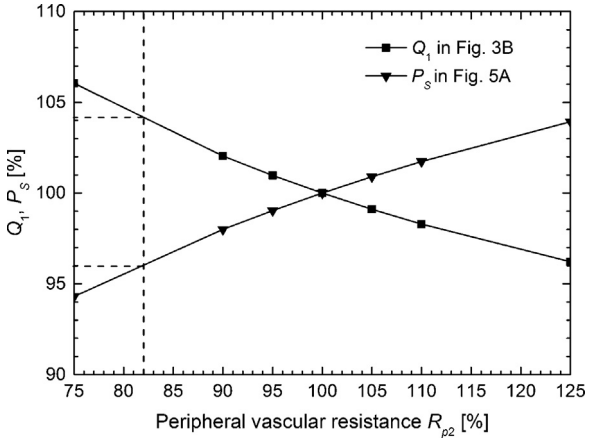

Fig. 8 – Contribution of peripheral vascular resistance of the left arm, R_{p2}, to cardiac output, Q_1, and supply pressure, P_S. P_S is fixed in Fig. 3B and Q_1 is fixed in Fig. 5A.

can be adopted to explain the change in the flow volume by regulation of the peripheral vascular resistance.

4.3. *Influence of upstream boundary condition on hemodynamics*

The amount of change in Q_2 was same as that in Q_1 for the pressure boundary condition, that is, both of them increased by 3.67×10^{-6} m^3/s when R_{p2} decreased by 25% in Fig. 3B. By contrast, the absolute value of the amount of the change in Q_2 was the same as that in the sum of Q_3 and Q_4, that is, Q_2 increased by 3.83×10^{-6} m^3/s and $Q_3 + Q_4$ decreased by the same amount when R_{p2} decreased by 25% in Fig. 5B. As for the pressure distribution, although the change in R_{p2} influenced only P_2 under the pressure boundary condition, as shown in Fig. 3A, it influenced all the pressures under the flow-volume boundary condition and their magnitudes were much larger than the pressure boundary condition.

As shown in Table 5, CI increased by 1.7% and the mean BP decreased by 2.2% when SVRI decreased by 4.3% at 180 seconds after the stimulation, although they had no statistical significance. In this study, a 4% decrease in SVR corresponds to an 18% decrease in peripheral vascular resistance, as shown in Fig. 6. This results in an increase of approximately 4% in Q_1 for the pressure boundary condition and a decrease of about 4% in P_S for the flow-volume boundary condition, as shown in Fig. 8. Either of these trends matches the experimental results by Takayama et al[11] with respect to the change in SVR. By contrast, however, P_S and Q_1 for each simulation cannot be changed because they were given as the boundary condition. Therefore, at present, we cannot conclude which boundary condition is appropriate, and thus, measurement of blood flow in another limb (e.g., a leg) is necessary to discuss it from the viewpoint of the area of the influence of R_{p2} within the arterial system.

4.4. *Limitations*

The findings of this study were in agreement with the experimental data[11] with respect to the relationships of Q_2 versus SVR, and Q_1 or P_S versus SVR. Because of limited available quantitative clinical data, however, the validity of the present model was limited to the value of Q_1 at the control condition under the pressure boundary condition, which was in the physiological range of the systemic circulation, and to satisfaction of the mass conservation at the present state. Thus, the authors are applying this model to hemodynamic change by stimulation of Zusanli (ST-36)[13] to further ensure its validity.

Takayama et al[11] have discussed the physiological relationship between the stimulation of Taichong and change in the blood flow volume. They argued that the sympathetic

Table 5 – Change in hemodynamics measured by Takayama et al.[11]

Parameter	Time course				
	Before	During	After 30 s	After 60 s	After 180 s
Flow volume in radial artery	100	47.1*	105.9	121.6†	119.6 (+19.6%)†
Flow volume in brachial artery	100	76.7†	105.5	108.2	119.2 (+19.2%)†
Mean arterial pressure	100				97.8 (–2.2%)
Cardiac index	100				101.7 (+1.7%)
Systemic vascular resistance index	100				95.7 (–4.3%)†

The data were reproduced from the report by Takayama et al.[11]
* $p < 0.01$ versus before acupuncture.
† $p < 0.05$.

nervous system is involved in this change via regulation of the peripheral vascular resistance, but this is still a hypothesis. The present analysis is based on the hypothesis that the change in the resistance is induced by stimulation. It is known that physical stimulation of an acupoint in different ways or even stimulation of different acupoints has the same efficacy although a difference in efficiency remains.[13,31–33] Therefore, it is presumed that not only the peripheral nervous system, but also the central nervous system and endocrine system are involved in signal transduction of the stimulation. Elucidation of the correlation will be introduced in a future work.

Hemodynamic change in the whole body by therapy is sometimes discussed based on partial hemodynamic change observed at limited sites, assuming that the observed change occurs equally in the whole body. This is considered to be due to the difficulty in simultaneous measurement of the changes in blood flow in the whole body resulting from the therapy. The present model has a potential to emulate the changes in blood distribution by acupuncture therapy for elucidation of the mechanism of the therapy by incorporating correlation of stimulation of an acupoint and response of physiological parameters affecting the hemodynamics.

Conflicts of interest

All contributing authors declare no conflicts of interest.

REFERENCES

1. Chen K, Xu H. The integration of traditional Chinese medicine and Western medicine. *Eur Rev* 2003;11:225–35.
2. Witt CM, Jena S, Brinkhaus B, Liecker B, Wegscheider K, Willich SN. Acupuncture for patients with chronic neck pain. *Pain* 2006;125:98–106.
3. Witt C, Brinkhaus B, Jena S, Linde K, Streng A, Wagenpfeil S, et al. Acupuncture in patients with osteoarthritis of the knee: a randomised trial. *Lancet* 2005;366:136–43.
4. Linde K, Streng A, Jürgens S, Hoppe A, Brinkhaus B, Witt C, et al. Acupuncture for patients with migraine: a randomized controlled trial. *JAMA* 2005;293:2118–25.
5. Melchart D, Streng A, Hoppe A, Brinkhaus B, Witt C, Wagenpfeil S, et al. Acupuncture in patients with tension-type headache: randomised controlled trial. *BMJ* 2005;331:376–82.
6. Brinkhaus B, Witt CM, Jane S, Linde K, Streng A, Wagenpfeil S, et al. Acupuncture in patients with chronic low back pain: a randomized controlled trial. *Arch Intern Med* 2006;166:450–7.
7. Yamazaki T, Sato M, Yano T, Sakurai K, Niwa F, Imanishi J. Randomized controlled study on enhanced cognitive function with acupuncture and improvement in life style. *Kampo Med* 2012;63:229–37 [In Japanese with English abstract].
8. World Health Organization (WHO). Guidelines on basic training and safety in acupuncture. Geneva, Switzerland: WHO; 1999. Available from: http://apps.who.int/medicinedocs/en/d/Jwhozip56e/. Accessed February 4, 2015.
9. Xu X. Acupuncture in an outpatient clinic in China: a comparison with the use of acupuncture in North America. *South Med J* 2001;94:813–6.
10. Takayama S, Iwasaki K, Watanabe M, Kamiya T, Hirano A, Matsuda A, et al. The present state of integrative medicine at four medical facilities in Germany. *Kampo Med* 2012;63:275–82 [In Japanese with English abstract].
11. Takayama S, Seki T, Watanabe M, Monma Y, Yang SY, Sugita N, et al. Brief effect of acupuncture on the peripheral arterial system of the upper limb and systemic hemodynamics in humans. *J Altern Complement Med* 2010;16:707–13.
12. Seki T, Watanabe M, Takayama S. Blood flow volume as an indicator of the effectiveness of traditional medicine. In: Saad M, editor. *Acupuncture: concepts and physiology*. Rijeka, Croatia: InTech; 2011:113–36.
13. Watanabe M, Takayama S, Yamamoto Y, Nagase S, Seki T, Yaegashi N. Haemodynamic changes in the superior mesenteric artery induced by acupuncture stimulation on the lower limbs. *Evid Based Complement Alternat Med* 2012;2012, doi:10.1155/2012/908546.
14. Low PA, Neumann C, Dyck PJ, Fealey RD, Tuck RR. Evaluation of skin vasomotor reflexes by using laser Doppler velocimetry. *Mayo Clin Proc* 1983;58:583–92.
15. Omura S. Pathophysiology of acupuncture treatment: effect of acupuncture on cardiovascular and nervous systems. *Acupunct Electrother Res* 1975;1:55–141.
16. Fung Y. *Biomechanics: circulation*. 2nd ed. New York: Springer; 1997, 34–36 and 108–13.
17. Stergiopulos N, Young DF, Rogge TR. Computer simulation of arterial flow with applications to arterial and aortic stenoses. *J Biomech* 1992;25:1477–88.
18. Wang JJ, Parker KH. Wave propagation in a model of the arterial circulation. *J Biomech* 2004;37:457–70.
19. Blackman BR, Gracía-Cardeña G, Gimbrone Jr MA. A new *in vitro* model to evaluate differential responses of endothelial cells to simulated arterial shear stress waveforms. *J Biomech Eng* 2002;124:397–407.
20. Cooney DO. *Biomedical engineering principles: an introduction to fluid, heart, and mass transport processes (biomedical engineering & instrumentation series) (translated by Gondo S)*. Tokyo: IPC; 1984:29–31 [In Japanese].
21. Narumi K, Nakanishi T, Shirai A, Hayase T. Development of one-dimensional mathematical model for validation of pulse diagnosis. *Trans Jpn Soc Mech Eng Ser B* 2008;74:142–8 [In Japanese with English abstract].
22. Shirai A, Nakanishi T, Hayase T. Numerical analysis of one-dimensional mathematical model of blood flow to reproduce fundamental pulse wave measurement for scientific verification of pulse diagnosis. *J Biomech Sci Eng* 2011;6:330–42.
23. Oka S. *Biorheology*. Tokyo, Japan: Shokabo Publishing Co. Ltd.; 1984:31–6 [In Japanese].
24. Suga H, Takaki M, Goto Y, Sunagawa K. *Cardiac mechanics and energetics*. Tokyo: Corona Publishing Co. Ltd.; 2000:38 [In Japanese].
25. Brandfonbrener M, Landowne M, Shock NW. Change in cardiac output with age. *Circulation* 1955;12:557–66.
26. Christie J, Sheldahl LM, Tristani FE, Sagar KB, Ptacin MJ, Wann S. Determination of stroke volume and cardiac output during exercise: comparison of two-dimensional and Doppler echocardiography, Fick oximetry, and thermodilution. *Circulation* 1987;76:539–47.
27. Sugawara J, Tanabe T, Miyachi M, Yamamoto K, Takahashi K, Iemitsu M, et al. Non-invasive assessment of cardiac output during exercise in healthy young humans: comparison between model flow method and Doppler echocardiography method. *Acta Physiol Scand* 2003;179:361–6.
28. Groeneveld AB, Nauta JJ, Thijs LG. Peripheral vascular resistance in septic shock: its relation to outcome. *Intensive Care Med* 1988;14:141–7.

29. Suehiro K, Tanaka K, Funao T, Matsuura T, Mori T, Nishikawa K. Systemic vascular resistance has an impact on the reliability of the Vigileo-FloTrac system in measuring cardiac output and tracking cardiac output changes. *Br J Anaesth* 2013;111:170–7.
30. Guyton AC, Hall JE. Local and humoral control of blood flow by the tissues. In: Textbook of medical physiology. 11th ed. Tokyo: Elsevier, Japan; 2010: 203–212 [In Japanese].
31. Seki T, Kurusu M, Tanji H, Arai H, Sasaki H. Acupuncture and swallowing reflex in poststroke patients. *J Am Geriatr Soc* 2003;51:726–7.
32. Akamatsu C, Ebihara T, Ishizuka S, Fujii M, Seki K, Arai H, et al. Improvement of swallowing reflex after electrical stimulation to lower leg acupoints in patients after stroke. *J Am Geriatr Soc* 2009;57:1959–60.
33. Takayama S, Seki T, Watanabe M, Takashima S, Sugita N, Konno S, et al. Changes of blood flow volume in the superior mesenteric artery and brachial artery with abdominal thermal stimulation. *Evid Based Complement Alternat Med* 2011;2011:214089, doi:10.1093/ecam/nep110.